104 (2025) 105887

Contents lists available at ScienceDirect

Poultry Science

journal homepage: www.elsevier.com/locate/psj

Full-Length Article

Thermal stability of multi-tier layer hen housing with all-year sidewall inlet ventilation system

Y.J. Chen [a], S.Z. Deng [a], Y. Wang [a,b,c], C. Liu [a], W.X. Qin [a], Y.X. Wei [d], Q. Tong [a,b,c], B.M. Li [a,b,c], W.C. Zheng [a,b,c,*]

[a] Department of Agricultural Structure and Environmental Engineering, College of Water Resources and Civil Engineering, China Agricultural University, Beijing 100083, China;
[b] Key Laboratory of Agricultural Engineering in Structure and Environment Ministry of Agriculture and Rural Affairs, Beijing 100083, China;
[c] Beijing Engineering Research Center on Animal Healthy Environment, Beijing 100083, China
[d] Institute of Animal Husbandry, Henan Academy of Agricultural Sciences, Zhengzhou, 450002, China

ARTICLE INFO

Keywords:
Laying hen
Ventilation
Multi-tier system
Thermal environment
Welfare

ABSTRACT

Large temperature fluctuations in alternative hen housing threaten poultry welfare and productivity because of temporary and seasonal ventilation adjustments. This study proposes an all-year sidewall inlet ventilation (**ASV**) system with buffer spaces and constant air inlet to stabilize the incoming airflow and minimize thermal variations at the hen level. The ASV system was evaluated in a commercial multi-tier layer house housing 24,000 hens in a temperate monsoon climate. Over 407 days, 58 sensors monitored outdoor conditions, buffer spaces, sidewall inlets, and indoor zones (between/within colony rows), with egg production and feed intake recorded. Results indicated without supplementary heating, indoor air temperatures ranged from 18.3 to 29.8°C, while outdoor temperature fluctuated from -22.0 to 37.3°C. The diurnal temperature fluctuation indoors remained within 3°C for 77.4 % of the period, peaking at 4.7°C. Average diurnal fluctuations indoors were 2.4°C (winter), 2.0°C (transition season), and 2.8°C (summer), compared to outdoors at 12.9°C, 14.0°C, and 11.6°C, respectively. During a 21.9°C outdoor diurnal fluctuation, variations in buffer spaces, sidewall inlets, and indoors measured 17.7°C, 12.2°C, and 4.7°C, showing significant gradation ($P < 0.05$). Summer indoor temperatures exceeded 26°C on 112 days due to cooling-activation at 28.0°C and reduced buffer space residence times. In the hottest month, interstitial zones between colony rows averaged 26.5 ± 1.29°C and 80 % ± 4.5 % RH. Microclimates within colony rows exhibited 1.5°C warmer and 9 % lower in RH than interstitial spaces ($P < 0.05$). Longitudinal temperature gradients peaked at the rear section, whereas lateral distributions were symmetric, with the middle column 0.7°C cooler than sides ($P < 0.05$). Diurnal feed intake deviation from the theoretical curve strongly correlated with 7-day mean, maximum, and minimum indoor temperatures ($P < 0.001$). In summary, the ASV system maintained indoor diurnal temperature fluctuation within 4.7°C across season, providing an effective ventilation strategy to support the transition to cage-free systems.

Introduction

Hens are homeothermic animals sensitive to cold and heat stress. The temperatures within layer houses are critical for their health, welfare, and productive performance, especially for modern high-yield laying hens (Dawkins et al., 2004; Barrett et al., 2019; Kim et al., 2023). It is generally recommended to maintain diurnal temperature fluctuations within 6°C, especially in the thermal neutral zone of 18-24°C. Exceeding this temperature range can lead to environmental stress (Al-Saffar and Rose, 2002; Tao, 2003; Lysenko et al., 2011). Wang (2020) further suggested that diurnal temperature fluctuations should ideally be limited to 3°C in enclosed poultry houses. Ventilation systems are crucial for maintaining a stable thermal environment, and tunnel ventilation is the most commonly used method (Bjerg et al., 2002; Lysenko et al., 2011). These systems require a lot of energy to maintain the desired temperature range. However, previous studies have shown that diurnal temperature fluctuations in tunnel-ventilated houses can exceed 8°C in a temperate monsoon climate (Wang, 2012; Hui et al.,

Appropriate scientific section: Management and Production

* Corresponding author.
E-mail address: weichaozheng@cau.edu.cn (W.C. Zheng).

https://doi.org/10.1016/j.psj.2025.105887
Received 11 March 2025; Accepted 22 September 2025
Available online 23 September 2025

2018; Wang et al., 2018a, 2019), resulting in lower feed conversion ratios compared to stable temperatures of 21°C or 23.9°C (Harris et al., 1974; Howlider and Rose, 1987; Al-Saffar and Rose, 2002; Tao, 2003). Nevertheless, the optimal operating mechanism by which ventilation affects the stable temperature regulation remains to be identified.

Weather conditions, building structure, and ventilation design can directly influence multiscale flow and heat transfer phenomena, with a subsequent effect on the temperature across different zones (Choi et al., 2024; Predicala and Maghirang, 2003; Tong et al., 2019; Zhao et al., 2013). Basically, a well-considered design of the building enclosure, including factors such as the building orientation, color of the external envelope, thickness of insulation materials, and bonding method of assembly panels, can significantly enhance thermal insulation performance and mitigate the impact of weather on the microclimate within layer houses (Garcimartin et al., 2007; Wang et al., 2018b). Moreover, various studies have suggested that incorporating an air buffer space, an air-recirculated ventilation system, or a double-duct ventilation system can improve the air intake temperature and reduce temperature fluctuations within the animal-occupied zone (Kim et al., 2022a; Kindangen et al., 2022; Yang et al., 2021; Yeo et al., 2019). These approaches offer a novel perspective for designing building-integrated ventilation, potentially contributing to the environmental sustainability of poultry farming. However, it should be noted that the above studies have mostly been conducted for simulation verification under specific temperature ranges and seasonal conditions.

The basic airflow trajectory within a ventilated house follows a path from the inlet to the exhaust fan (Randall and Battams, 1979). In present, common inlets include sidewall inlet and evaporative cooling pads. Cross-ventilation, which utilizes multiple exhaust fans and sidewall inlets, is commonly adopted during the winter and transition seasons (Kwon et al., 2015). In the summer, a tunnel or combi-tunnel ventilation system with evaporative cooling pads is typically used to create a wind chill effect. Evaporative cooling pads are installed on the gable wall and/or both sidewalls at one end of the building, and fans are installed at the opposite end (Cheng et al., 2018; Webster and Czarick, 2000). However, practical observations indicated that temporary and seasonal adjustments of ventilation modes based on external weather conditions cause significant temperature fluctuations and uneven temperature distribution (Xu, 2022). Furthermore, computational fluid dynamic (**CFD**) simulations conducted by Gebremedhin and Wu (2005) found that varying the air-inlet can cause significant variations in the uniformity of the flow-field and exacerbate turbulent pulsation within the houses. Therefore, we hypothesized that maintaining a consistent airflow path through a fixed configuration of air inlets and air outlets across different seasons may enhance thermal stability within layer houses.

Besides focusing on building structure and ventilation design, housing systems and stocking density present significant challenges in stable temperature regulation. This issue is particularly pertinent in light of the industry's ongoing transition to cage-free systems, which aim to address welfare concerns associated with caged housing. Al-Saffar and Rose (2002) noted that birds in cage-free housing often experience large diurnal fluctuations in air temperature, particularly in hot climates. Zhao et al. (2015) conducted a 27-month environmental monitoring study that compared conventional cages, enriched colony systems, and aviary houses. Their findings indicated that a cross-ventilated aviary house (49,842-hen capacity) exhibited poorer indoor air quality, higher ventilation rates, and greater supplemental heating demands under the synergistic coupling effects of increased hen activity levels and reduced stocking density. Similar conclusions were drawn by Li et al. (2020, 2023) and Hong et al. (2021), whose research focused on tunnel-ventilated aviary systems. Chen et al. (2021) employed CFD modeling to evaluate a "top-wall inlet sidewall exhaust" ventilation in a cage-free housing system under cold weather conditions (0°C). The simulation predicted that the house temperatures would range from 10 to 20°C at a stocking density of 0.11 m^2 per bird. However, this idealized assumption (birds are evenly distributed) contrasts with actual cage-free operations, where lower stocking densities facilitate greater horizontal and vertical mobility. This mobility markedly complicates the regulation of environmental factors (Rehman et al., 2018; Yang et al., 2024; Zhao et al., 2013). Therefore, this complexity highlights the critical need for purpose-designed ventilation systems and thorough performance evaluations tailored to the specific requirements of modern multi-tier poultry production systems.

In a previous study, our team investigated a longitudinal buffer space ventilation system in a conventional caged layer house with a capacity of 30,000 hens, situated in a temperate continental climate from May to June (Wang et al., 2018a). We utilized 42 spatially distributed monitoring points to demonstrate the effectiveness of the system in reducing dust deposition and mitigating diurnal temperature fluctuations. Based on these findings, the present study developed an all-year sidewall inlet ventilation (**ASV**) system featuring buffer spaces and constant air inlets. The performance was evaluated in a commercial multi-tier layer house throughout an entire production cycle, with regard to the flock performance and thermal environment under various seasonal and diurnal conditions in a temperate monsoon climate.

Materials and methods

Design of all-year sidewall inlet ventilation system

Firstly, the ASV system adopted a previously established longitudinal buffer space design (Wang et al., 2018a), which incorporates a transitional zone to mitigate the direct impact of external weather fluctuations on the incoming airflow. To determine the optimal geometry of this buffer space, the air within it was treated as a ventilated air layer (Säwén et al., 2021). Under the negative-pressure ventilation, this airflow was modeled as the forced flow of a Newtonian fluid with constant physical properties. Based on principles of energy and mass conservation (Sandberg and Moshfegh, 1998), the optimal width-to-height ratio (W/H) was consequently determined to be 0.35.

Secondly, the ASV system is designed to maintain a consistent airflow path via fixed inlet and outlet channels under all seasons and weather conditions. In this study, sidewall inlets were utilized as the sole constant air inlets due to their longer service cycle. To address high-temperature conditions, evaporative cooling pads were installed on the exterior wall of the buffer space to pre-cool the air entering through the sidewall inlets.

In summary, the ASV system ensures the airflow consistently follows this sequence (see Fig. 1): outdoor → evaporative cooling pad → buffer space (fully mixed) → sidewall inlet → hen-occupied zone → exhaust fan. This constant airflow path, combined with the thermal buffering capacity, is intended to mitigate the impact of external weather

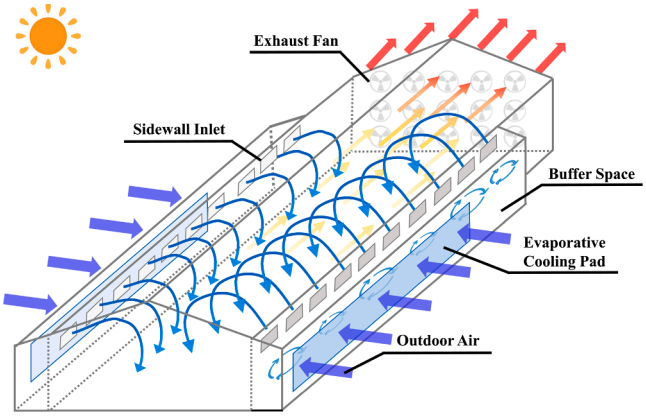

Fig. 1. Schematic diagram of the all-year sidewall inlet ventilation (ASV) system depicting the consistent airflow path and key components.

fluctuations and enhance the thermal stability within the layer houses.

Experimental layer house

This study was conducted in a commercial multi-tier layer house equipped with the ASV system, located in Beijing, China (40°19′ N, 117°23′ E) and constructed in 2023 (see Fig. 2).

Building characteristics

The east-west-oriented layer house measured 89 m (length) × 14 m (width) × 4.8 m (height). Two symmetrical buffer spaces (4.8 m high × 1.7 m wide × 78 m long) were installed along the longitudinal side of the building. The main walls of the layer house were constructed with a thickness of 150 mm using rock wool sandwich panels, while the buffer space walls were 50 mm thick. The roof featured a double-layer system composed of two 100 mm rock wool sandwich panels, and it was equipped with a suspended ceiling. The cladding panels of the entire building envelope were joined with a concealed fastener connection system to create a smooth interior surface without any protrusions. Additionally, critical gaps and joints were sealed with polyurethane foam to improve airtightness. Steel columns were placed outside the thermal insulation layer to prevent the formation of thermal bridges.

Ventilation system configuration

There were 14 gable-mounted exhaust fans with shutters and diffusers, including 12 constant-speed fans (1.8 kW, 47,800 m^3 h^{-1} capacity) and two variable-speed fans (0.75 kW, 23,300 m^3 h^{-1} capacity). On each longitudinal wall, 59 inlets with arc deflectors were installed. Each inlet had outline dimensions of 800 × 360 mm and installation dimensions of 770 × 340 mm. The inlet array spanned 62.3 m, with the first inlet positioned 0.2 m from the eastern gable and the lower edge of all inlets fixed 3.7 m above ground level. In addition, evaporative cooling pads (0.1 m thick × 1.5 m wide × 44 m long) were vertically installed on the exterior walls of both buffer spaces, protected by sunshades to mitigate rainwater intrusion and solar radiation.

Environmental control strategy

The ventilation operated in two modes: 1) Fresh air entered through the buffer spaces and sidewall inlets, circulating through the hen-occupied zone before being exhausted by the fans (normal mode); and 2) air passed through the wetted cooling pads before entering the buffer space (cooling mode, activated at indoor temperatures > 28.0°C). System operation was automated through an environmental control system (Rotem Pro, Munters Air Treatment Equipment Co., Ltd., Beijing, China), which regulated ventilation based on outdoor temperature, flock age (in weeks), and production level. The ventilation system was designed with minimum and maximum capacities of 0.63 m^3 h^{-1} and 15.93 m^3 h^{-1} per hen, respectively. A 30-stage fan control sequence was implemented with the sidewall inlet openings dynamically adjusted according to the fan stage activation and building static pressure.

Multi-tier housing system and birds

The study used 24,000 *Jing Ting No.6* laying hens (Beijing Huadu Yukou Poultry Industry Co., Ltd., Beijing, China). Hens were placed in the housing system at 12 weeks of age (23 September 2023) and depopulated at 70 weeks of age (2 November 2024), maintaining a stocking density of 0.064 m^2 per hen.

Multi-tier housing system

The system was designed and developed by the China Agricultural University (see Fig. 3). Hens were distributed in three parallel colony rows, each longitudinally divided by wire mesh screens into 11 pens. The spatial distribution of colony units followed an east-west gradient: pen 1 (8.4 m long × 2.8 m wide × 3.3 m high) contained seven full-colony units, whereas pens 2-11 (6.0 m long × 2.8 m wide × 3.3 m high) each contained five units, resulting in a total of 57 colony units per row. The multi-tier colony consisted of four tiers, with the fourth tier housing nest boxes. Each of the four tiers featured under-tier manure belts. External feed troughs and internal nipple drinkers were installed only on tiers 1-3 to mitigate health and welfare issues associated with high stocking density on the top tier (Fu, 2019; Yin et al., 2024). The second, third, and fourth tiers were equipped with galvanized steel perches (full length 6.0 m). Unlike the aviary system currently used in the European Union, there was no provision for litter on the floor. Hens within each pen could freely access all colony units and migrate between all tiers.

Management strategy

Laying hens were managed using an automated system. Feeding was

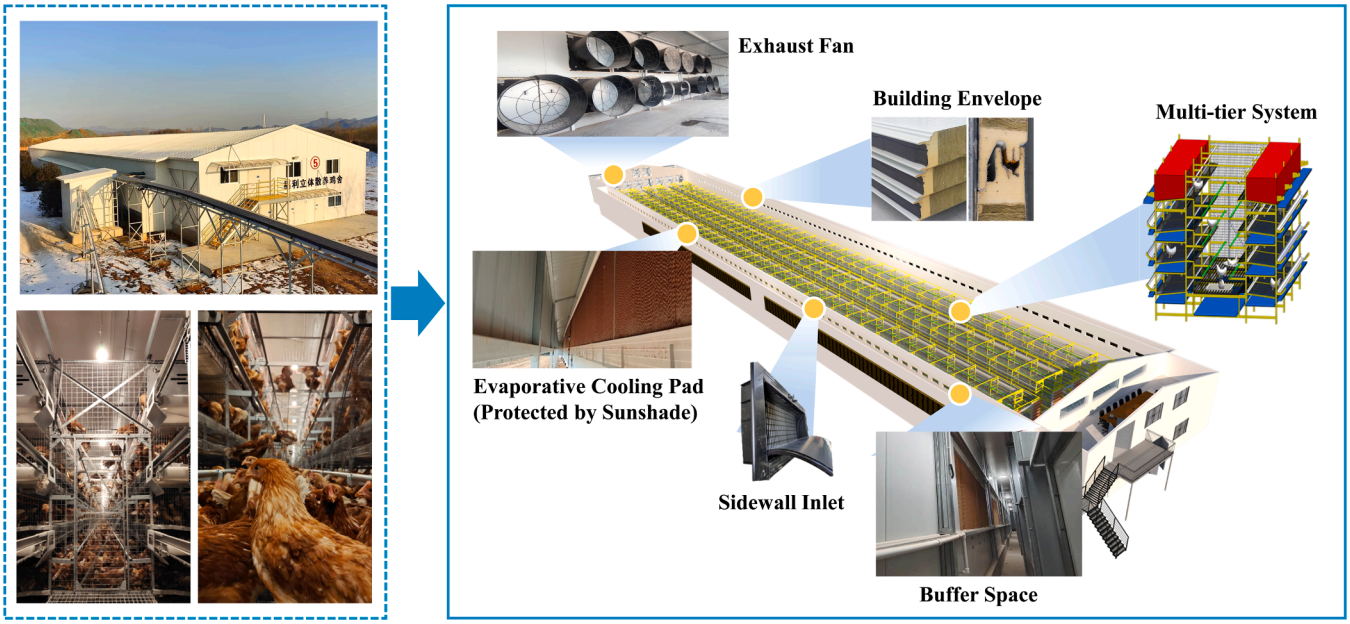

Fig. 2. Internal and external schematic drawings of the experimental multi-tier layer house with an all-year sidewall inlet ventilation system.

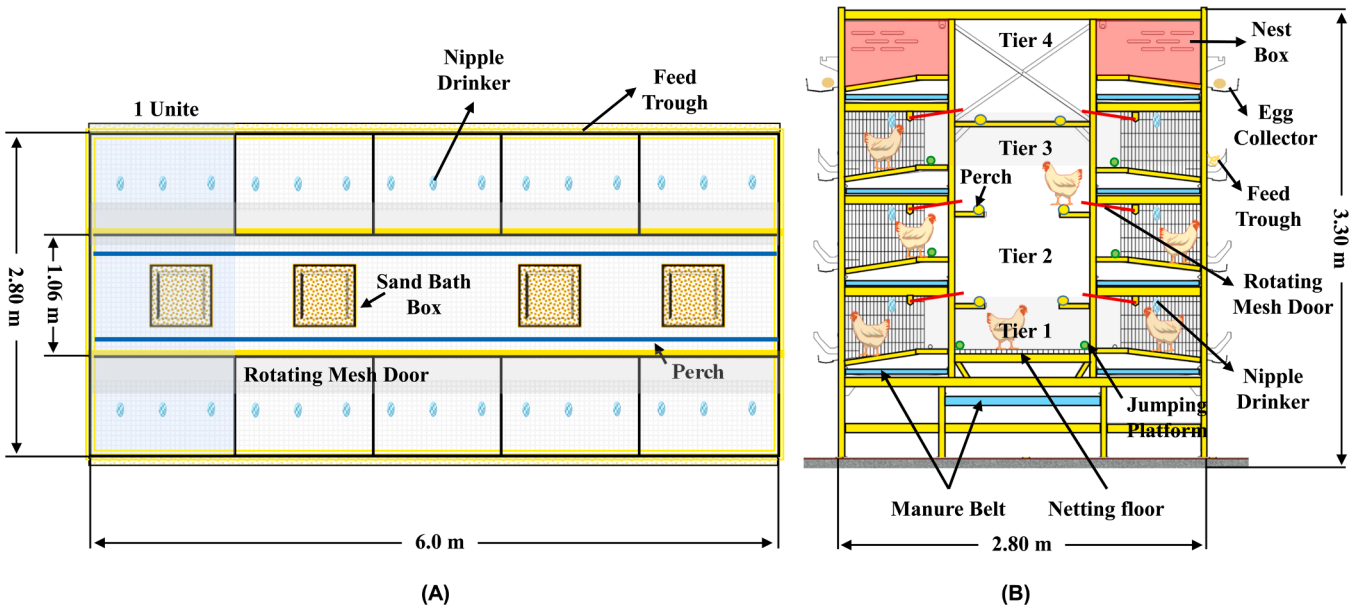

Fig. 3. Top view (A) and side view (B) schematic drawings of a pen in the multi-tier system.

performed three times daily, and water was provided ad libitum. The hens were fed a commercial corn-based diet (see Tab. 1), which was formulated based on egg production, feed intake, and ingredient cost according to five distinct phases. The photoperiod schedule, managed according to standard commercial protocols, is listed in Tab. 2. From 12 weeks of age, the photoperiod was gradually increased from a 10-h light and 14-h dark schedule to a 16L:8D schedule over 30 weeks. From weeks 48 to 59, the lights were turned on for one hour between 23:00 and 24:00. This strategy was designed to encourage feed intake and support productive performance during a period of high ambient temperatures. A centralized egg collection system was used for daily egg collection. Manure belt removal was performed every 1-2 days, with the manure subsequently stored in on-farm facilities.

Measurement of thermal environment

Continuous thermal environment monitoring was conducted throughout the production cycle, from September 23, 2023, to November 2, 2024. The spatial distribution of the monitoring points is illustrated in Fig. 4, which shows both the top and side views of the sensor placements.

Table 1
Changes in nutrient composition of commercial layer diet throughout a production cycle.

Nutrient	Pullet (12-14 wk of age)	Pre-lay (15-20 wk of age)	Peak (21-30 wk of age)	Peak (31-56 wk of age)	Post-peak (57-70 wk of age)
Metabolizable Energy (kcal/kg)	2734	2710	2657	2641	2629
Crude Protein (%)	15.50	16.20	17.20	15.50	15.30
Crude Fiber (%)	8.00	7.00	7.00	7.00	7.00
Calcium (%)	0.80	2.60	3.70	3.73	3.97
Available Phosphorus (%)	0.42	0.50	0.44	0.37	0.36
Na (%)	0.36	0.36	0.32	0.32	0.32
DLys (%)	0.68	0.74	0.81	0.68	0.65
DMet (%)	0.33	0.42	0.40	0.36	0.33
DMet+DCys (%)	0.67	0.76	0.80	0.71	0.65
DThr (%)	0.47	0.54	0.54	0.47	0.43

Table 2
Photoperiod schedule and light intensity for the experiment layer house during the entire production cycle.

Duration (week)	Photoperiod Schedule		Light Intensity[1] (lux)
12~14	10L:14D	07:00~17:00	15
15~16	10L:14D	07:00~17:00	25
17	10L:14D	04:00~14:00	
18	11L:13D	04:00~15:00	
19	12L:12D	04:00~16:00	
20	12.5L:11.5D	04:00~16:30	
21	13L:11D	04:00~17:00	
22	13.5L:10.5D	04:00~17:30	
23	14L:10D	04:00~18:00	
24~25	14.5L:9.5D	04:00~18:30	
26~27	15L:9D	04:00~19:00	
28~29	15.5L:8.5D	04:00~19:30	30
30~47	16L:8D	04:00~20:00	
48~59		04:00~20:00, 23:00~24:00	
60		04:00~20:00, 23:00~23:45	
61		04:00~20:00, 23:00~23:30	
62		04:00~20:00, 23:00~23:15	
63~70		04:00~20:00	

[1] The light intensity was measured at the feeder.

Fifty-eight Hobo Pro Series air temperature and relative humidity loggers (Onset Computer Corp., Bourne, MA, USA) were strategically deployed to measure outdoor, buffer space, sidewall inlet, and indoor environments (between and within colony rows). The dataloggers of interstitial zones between colony rows were installed in the following directions to characterize three-dimensional thermal profiles: 1) longitudinal measurements, which included three sensor distances from the gable wall (without fans), at 17 m (front), 41 m (middle), and 65 m (rear); 2) lateral measurements, which included three aisles across Column 1, Column 2, and Column 3; 3) vertical measurements, which included four heights of 1.25 m (Tier 1), 2.05 m (Tier 2), 2.85 m (Tier 3), and 3.65 m (Tier 4), corresponding to the hen breathing heights. Additionally, nine sensors were installed within the colony rows at a height of 2.85 m, according to the aforementioned horizontal orientations, to reflect the microclimate at the hen level more accurately.

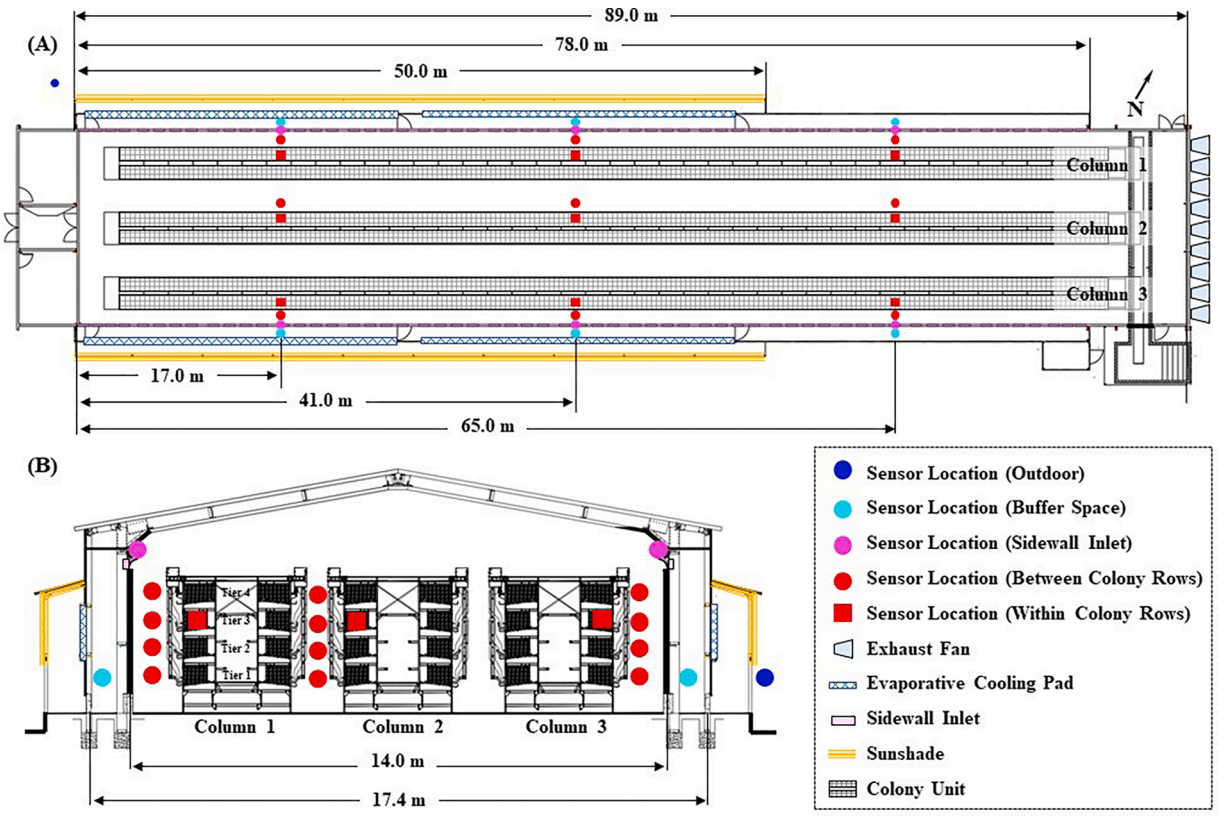

Fig. 4. Schematic of the layer hen house showing the floor plan (A) and the cross-sectional view (B) of the house layout, ventilation system, and sensor locations for the temperature and relative humidity.

Twelve sensors were installed in the buffer space and sidewall inlet, corresponding to the three longitudinal sections mentioned above. One sensor was placed outside to measure ambient conditions.

These loggers performed within a temperature range of −40 to 70°C and measured relative humidity from 0 % to 100 %, with an accuracy of ± 0.2°C and ± 3 %, respectively. Each measurement was recorded at 5-minute intervals. All measurements were recorded without interference from commercial production. Additionally, all data loggers deployed in this study were checked and calibrated using a National Institute of Standards and Technology-certified Heating and Cooling Temperature Calibrator (CL134-1; OMEGA Engineering, Inc., Norwalk, CT, USA) before and approximately every 4 weeks during the experiment.

Measurement of production performances

Data on the daily number of eggs, feed consumption, and dead hens were recorded from 79 (12 weeks) to 485 days (70 weeks) of age. Hen-day egg production (%) was calculated as the daily number of eggs divided by the number of live hens on the same day. The ages at which the flock reached 50 % (onset of lay) and peak hen-day egg production were determined based on these daily records. Daily feed intake (g^{-1} hen^{-1}) was calculated by dividing the total daily feed consumption by the number of live hens. The typical egg production and feed intake curves for *Jing Ting No.6* laying hens (from 12 to 70 weeks of age), as provided in the breeder's management guide, were used as a reference for comparison.

Data and statistical analysis

All statistical analyses were performed using IBM SPSS Statistics (version 25.0; SPSS Inc., Chicago, IL, USA), and graphs were created using OriginPro (Origin Lab, Northampton, MA, USA). This study used diurnal temperature fluctuation as the metric to assess thermal stability. Thermal distribution was characterized by the mean ± SD at different locations. Pearson correlation analysis was used to evaluate the association between temperature and egg production, as well as feed intake. Significance levels were denoted as follows: $*P < 0.05$, $**P < 0.01$, and $***P < 0.001$.

Thermal stability

It was first evaluated by plotting a line graph of the daily mean, maximum, and minimum temperatures, as well as a bubble graph of diurnal temperature fluctuation, for both the outdoor and indoor environments (monitored via 36 sensors between colony rows) across the entire production cycle. The ASV system was further assessed by analyzing diurnal temperature fluctuations under different seasons and weather conditions, as detailed below:

1) Seasonal lengths and onsets were determined according to the GB/T 42074-2022 "Division of Climatic Seasons" standard (Chen et al., 2022), using 5-day outdoor moving average temperatures obtained from the National Meteorological Information Center. Fixed thresholds defined in the national standard were applied: 22°C for summer and 10°C for winter. This classification enabled a detailed evaluation of the range of diurnal temperature fluctuations controlled by the ASV system across seasons.
2) To evaluate system performance under extreme weather conditions, weeks containing the day with the highest outdoor temperature fluctuation (11 April-17 April) and the day with the highest outdoor temperature (4 July-10 July) were selected separately for each operational mode (normal and cooling). During these periods, diurnal temperature fluctuations were analyzed at different structural levels: outdoors, buffer spaces, sidewall inlets, and indoors.

Thermal distribution

The thermal environment distribution within multi-tier systems

remains rarely characterized. The month with the highest diurnal temperature fluctuation, as identified in the previous section, was selected for detailed analysis of temperature and humidity conditions along the longitudinal, lateral, and vertical directions, as well as inside and outside the colony rows. These data provide foundational information for optimizing ventilation strategies.

Flock performance

Changes in egg production and feed intake over the entire cycle were plotted against both hen age and indoor air temperature, alongside the typical performance curve provided for the genetic strain of the laying hens. Furthermore, Pearson correlation analysis was conducted to examine the relationship between the deviation of actual production performance from theoretical values and the corresponding 7-day average daily temperature, daily minimum temperature, daily maximum temperature, and diurnal temperature fluctuation.

Results and discussion

Thermal performance over the production cycle

Fig. 5 illustrates the variations in the indoor, target room, and outdoor temperatures over 407 consecutive days (23 September 2023 to 2 November 2024). The outdoor temperature exhibited substantial fluctuations from −22.0 to 37.3°C, averaging of 12.5 ± 12.14°C. Under these conditions, the indoor temperatures ranged from 18.3 to 29.8°C, with an average of 23.1 ± 2.36°C, fluctuating around the target room temperature, without supplementary heating.

Comparing it with the operational ranges reported in other aviary systems. Oliveira et al. (2020) observed that temperatures within fan banks and hallways ranged from 20.3 to 30.9°C, while the ambient temperature varied from 3.4 to 28.9°C, with a floor space of 0.064 m^2 per bird. Zhao et al. (2015) surveyed air temperature during a complete production cycle. They reported an average temperature of 26.9 ± 1.2°C at hen level, compared with 9.9 ± 10.6°C at the ambient level, with a floor space of 0.066 m^2 per bird. Their target temperature was 25.6°C, and supplemental heating was triggered at 22.8°C. Similarly, Hayes et al. (2013) monitored temperatures ranging from 19 to 32°C (four sensors near fans) over 19 months in Iowa, USA. However, direct comparisons of absolute temperature ranges are of limited value due to differences in climate conditions, targeted temperature, sensor layout, stocking density, and especially supplementary heating. Furthermore, in the absence of a side-by-side comparison with a traditional ventilation system in this study, a more insightful approach is combined with examining the environment's short-term stability, which is less influenced by absolute set points and more reflective of the system's performance to buffer external disturbances.

Thermal performance on the seasonal scale

Exploring the applicability of the ASV system across different seasons was a core objective of this study. Over the 407 days, seasonal distribution based on outdoor temperature was as follows: winter (128 days), summer (136 days), autumn (88 days, in two segments), and spring (55 days). Seasonal outdoor and indoor temperature statistics are summarized in Table 3.

In winter, the indoor temperature ranged from 18.3 to 24.3°C, averaging 21.2 ± 0.93°C, while the outdoor temperature ranged from −22.0 to 17.4°C, with an average of −0.4 ± 8.55°C. These results were achieved under minimal ventilation (0.63 $m^3\ h^{-1}$ per bird) and no supplemental heating. During the transitional seasons, indoor temperatures ranged from 19.2 to 27.6°C, averaging 22.1 ± 1.78°C, whereas outdoor temperatures showed a wider range, from −3.1 to 29.7°C, with an average of 13.8 ± 7.10°C. In summer, indoor temperatures ranged from 20.4 to 29.8°C, with an average of 25.3 ± 1.92°C, while outdoor temperatures ranged from 6.2 to 37.3°C, with an average of 25.0 ± 6.07°C.

The optimal temperature range for laying hen productivity and welfare is 18-26°C (Garcimartin et al., 2007; Olgun et al., 2007; Wang, 2020). The ASV system maintained temperature within this range for 295 days (72.5 % of the study period), primarily during winter and transitional seasons. This performance can be attributed to the enhanced building envelope tightness, effective insulation, and thermal buffering

Table 3
Seasonal statistical summary of indoor and outdoor temperatures.

Seasons	Locations	Temperature (°C)			
		Average	Maximum	Minimum	Standard Deviation
Winner	Outdoor	−0.4	17.4	−22.0	8.55
	Indoor	21.2	24.3	18.3	0.93
Transitional Season	Outdoor	13.8	29.7	−3.1	7.10
	Indoor	22.1	27.6	19.2	1.78
Summer	Outdoor	25.0	37.3	6.2	6.07
	Indoor	25.3	29.8	20.4	1.92

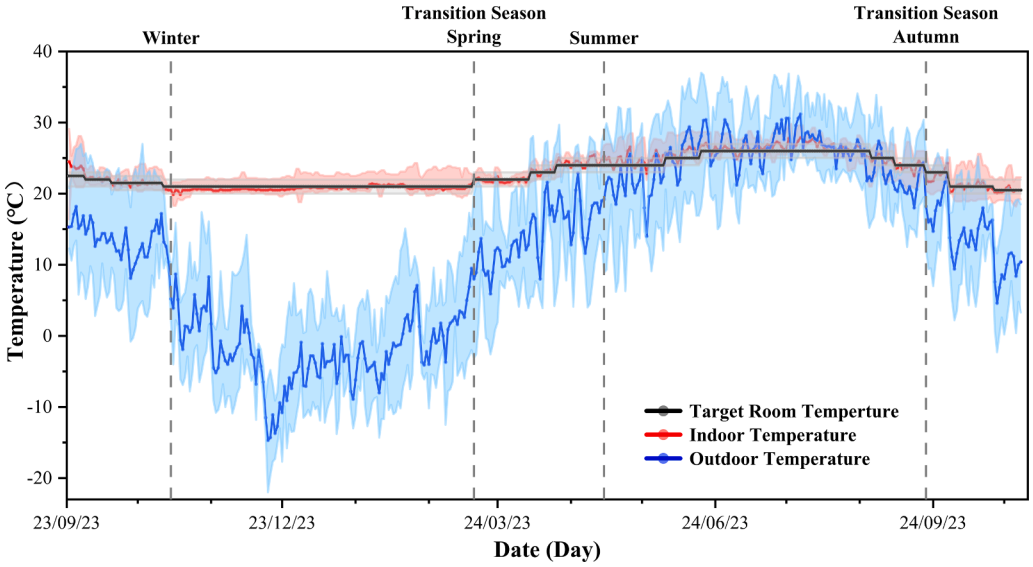

Fig. 5. Daily outdoor, indoor, and targeted room temperatures of the multi-tier system throughout a production cycle (407 consecutive days).

capabilities.

Unlike conventional negative-pressure buildings, which lose heat directly through their envelope, the ASV system establishes a stable conductive gradient: Warm Indoor Air → Inner Wall → Buffer Space Air → Outer Wall → Outside. This reduces the thermal difference across the main building envelope. In winter, incoming cold air is pre-warmed as it lingers in the buffer space and circulates over the warm inner wall surface before entering the animal-occupied zone. Turner et al. (2022) reported higher liquefied petroleum gas consumption (5.890 L per tonne of eggs) in Canadian multi-tier layer houses compared with conventional cages (0.079 L per tonne of eggs). Therefore, the ASV system may lead to net positive outcomes in cold weather by passively pre-warming incoming air through structural design.

However, exceedances above 26°C occurred on 112 days (27.5 % of the period), mainly in summer. This highlights a limitation under high heat load conditions. While the cooling activation threshold was intentionally set to 28.0°C to assess passive resilience, future operational iterations could optimize this set point. Further research is also warranted to monitor the wind chill effects of the ASV system.

Stability performance with diurnal temperature fluctuation

The diurnal temperature fluctuation was used as the thermal stability coefficient, where a lower value indicated greater stability in the thermal environment (Albright and Scott, 1974; Han et al., 2024). Fig. 6 illustrates the diurnal temperature fluctuations inside and outside the house over a year. The indoor diurnal fluctuation ranged from 0.7 to 4.7°C, with an annual mean of 2.5°C, compared to an outdoor range of 1.3 to 21.9°C and a mean of 12.8°C.

Seasonal analysis further demonstrated the system's effectiveness. In winter, the average indoor temperature fluctuation was 2.4°C, ranging from 1.2°C to 3.9°C. Outdoors, the average diurnal fluctuation was 12.9°C, with values ranging from 2.1°C to 20.3°C. During the transitional seasons, indoor fluctuations averaged 2.1°C, varying between 0.7°C and 4.0°C, while the average outdoor fluctuation was 14.0°C, with a range of 3.2°C to 21.9°C. In summer, the average indoor fluctuation increased to 2.8°C, with a span from 0.9°C to 4.7°C, compared to an outdoor average of 11.6°C and fluctuations ranging from 1.3°C to 21.8°C.

The increased variability observed in summer is primarily attributable to higher ventilation rates, which reduce air residence time within the buffer space and diminish its thermal buffering capacity, as Ruzal et al. (2011) noted. This led to greater susceptibility to transient cooling effects and infiltration of ambient conditions.

Throughout the study, it was observed that the indoor diurnal temperature variation remained within 3°C on 77.4 % of days and never exceeded 4.7°C, regardless of seasonal or weather changes typical of a temperate monsoon climate, thereby achieving a primary goal of environmental control, which helps ensure the health and productivity of hens (Mueller 1961; Al-Saffar and Rose, 2002). The temperature fluctuations were particularly stable during the winter and transitional seasons, consistently remaining below 4.0°C. However, real-time changes in ventilation rates and static pressure (Chen et al., 2016; Zhao et al., 2015), important parameters for optimizing the ASV system, particularly during summer, were not monitored.

Stability performance under extreme weather conditions

The efficacy of the ASV system was critically assessed under two characteristic extreme weather scenarios: a period of maximum diurnal fluctuation (normal mode) and a period of peak heat (cooling mode).

Normal mode

Fig. 7A illustrates the temperature variations across different building levels during the week containing the maximum daily ambient fluctuation. Throughout this week, the outdoor temperature fluctuated significantly, ranging from 4.2 to 27.1°C. This wide range is due to the low specific heat capacity of dry air, which leads to rapid temperature changes during Beijing's transitional seasons (Luo et al., 2021). As shown in Fig. 7B, there were significant differences in temperatures across all building levels ($P < 0.05$). The standard deviation of weekly temperature progressively decreased across these structural boundaries: 5.06°C (outdoor), 4.56°C (buffer space), 3.15°C (sidewall inlet), and 1.37°C (indoor). This trend highlights a strong buffering effect on thermal variability, underscoring the critical role of the buffer space. This finding aligns with prior reports of reduced temperature fluctuations in buffer spaces (Wang et al., 2018a).

The system's buffering capacity was clearly demonstrated on the day with the highest outdoor temperature fluctuation (16 April, 21.9°C). Diurnal temperature fluctuations were recorded at 17.7°C in the buffer

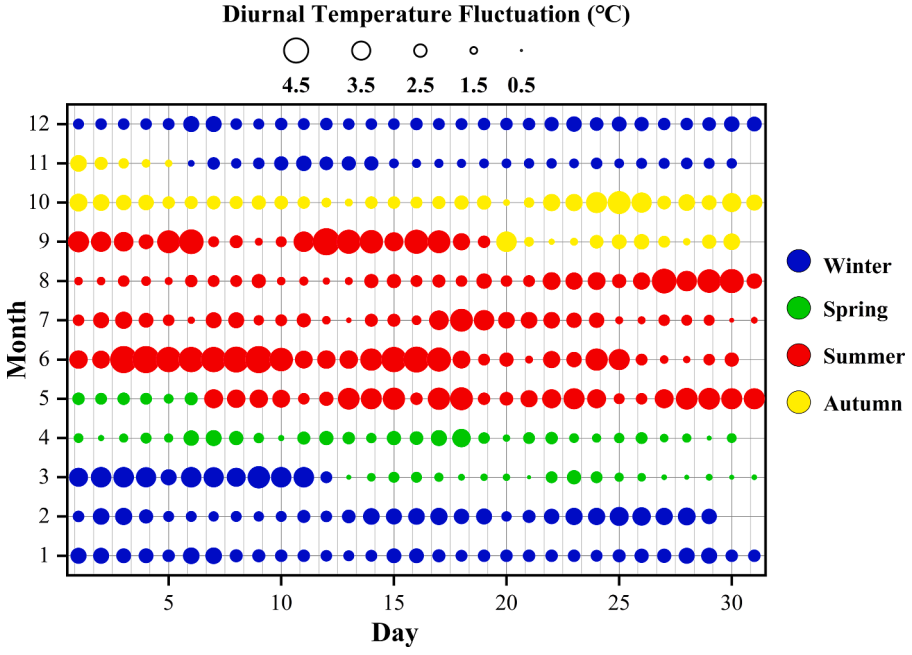

Fig. 6. Seasonal and annual patterns of indoor diurnal temperature fluctuation.

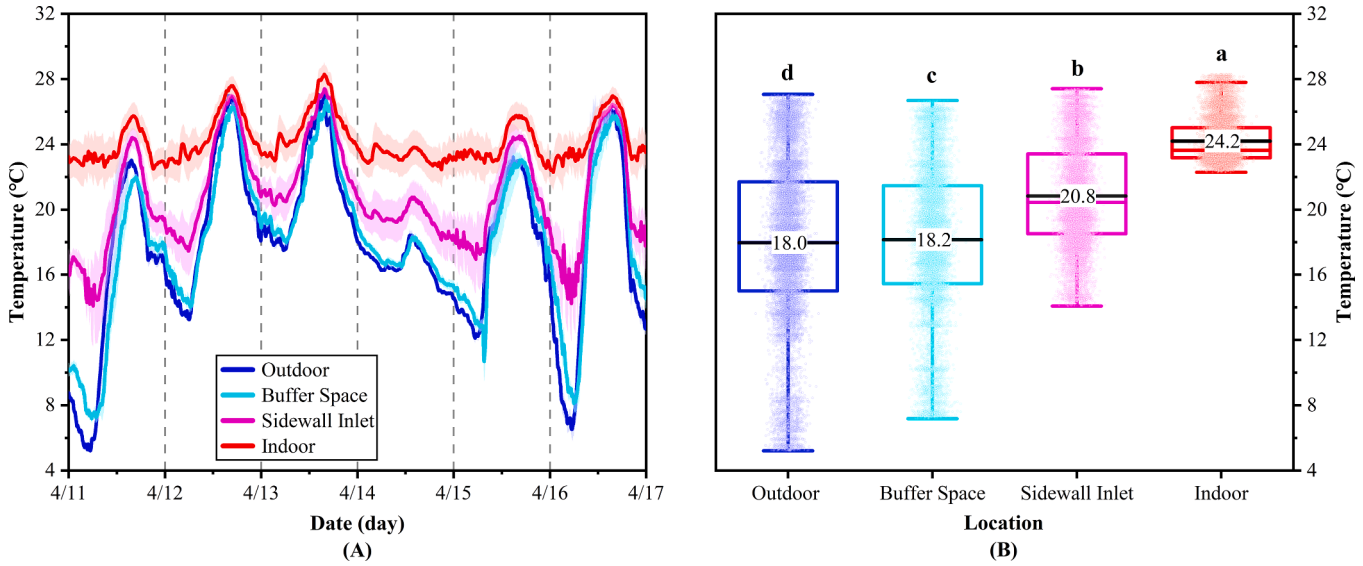

Fig. 7. (A) Temporal profile of outdoor, buffer space, sidewall inlet, and indoor average air temperatures of the multi-tier system from 11 April to 17 April 2024. (B) Distribution of weekly average temperatures measured outdoors, in the buffer space, at the sidewall inlet, and indoors. Different letters "a-d" within the box plot indicate that different locations had significantly different means ($P < 0.05$).

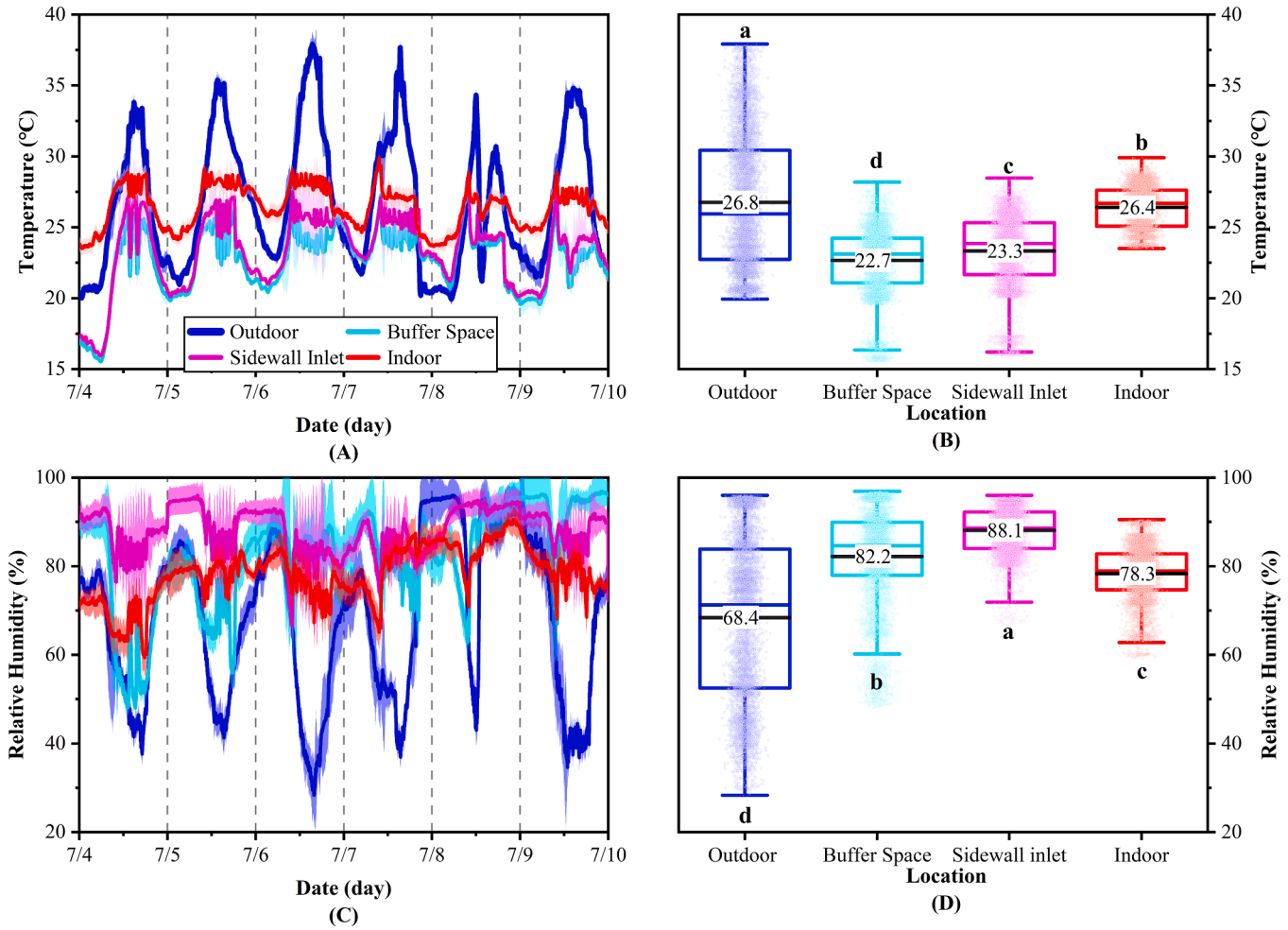

Fig. 8. Temporal profile of outdoor, buffer space, sidewall inlet, and indoor average air temperatures (A) and relative humidity (C) of the multi-tier system from 4 July to 10 July 2024. Distribution of weekly average temperatures (B) and relative humidity (D) measured outdoors, in the buffer space, at the sidewall inlet, and indoors. Different letters "a-d" within the box plot indicate that different locations had significantly different means ($P < 0.05$).

space, 12.2°C at the sidewall inlet, and only 4.7°C indoors. This progressive attenuation of external thermal shocks highlights the system's effectiveness in maintaining a stable hen-occupied environment despite severe external conditions.

Cooling mode

Fig. 8 illustrates the temperature and relative humidity across different building levels during the week containing the hottest ambient temperature. This week, outdoor temperatures ranged widely from 20.0 to 37.3 °C, while relative humidity fluctuated between 28 % and 96 %. Significant temperature and relative humidity differences were observed across all building levels ($P < 0.05$, Fig. 8B and 8D). Temperatures exhibited a clear gradient: outdoor temperatures averaged 26.8 ± 4.7 °C, decreasing to 22.7 ± 2.34 °C in the buffer space and 23.3 ± 2.52 °C at the sidewall inlets, before stabilizing at 26.4 ± 1.45 °C indoors. A similar progressive stabilization occurred in relative humidity, with outdoor relative humidity averaging 68 ± 18.3 %, increasing to 82 ± 11.2 % in the buffer space and 88 ± 5.0 % at the sidewall inlets, and moderating to 78 ± 6.0 % indoors. Cooling was primarily achieved through evaporative pads, which pre-cooled incoming air. However, the nearly overlapping temperature and humidity profiles between the buffer space and sidewall inlets indicate reduced air residence time within the buffer space under high ventilation rates, thereby diminishing its thermal buffering capacity.

On the hottest day recorded, with an outside temperature of 37.3°C and a relative humidity of 28.0 % ± 1.6 %, we evaluated the cooling efficiency of the evaporative pads. The maximum theoretical cooling achievable by these pads is based on the difference between the dry-bulb and wet-bulb temperatures (Hui et al., 2018). According to the enthalpy-humidity diagram, the outdoor wet-bulb temperature was found to be 22.6°C. The measured temperature in the buffer space, which approximates the temperature of the air after passing through the pads, was 23.9 ± 0.26°C. This indicates a high cooling efficiency of 91.2 %. The external sunshade structure significantly contributed by reducing solar radiation and preventing rainwater intrusion, which allowed the pads to operate close to their theoretical maximum efficiency.

In summary, the ASV system demonstrated effective thermal buffering against extreme diurnal temperature fluctuations and achieved high cooling efficiency under extreme high-temperature conditions. These results confirm its ability to maintain indoor thermal stability under various climatic challenges, supporting its applicability in sustainable, climate-resilient poultry production.

Thermal distribution of the multi-tier system

Analysis for this section focused on July to assess the most challenging thermal conditions. July was the hottest month and exhibited the largest indoor diurnal temperature fluctuation. The combination of heat stress and uneven environment during this period may present a substantial risk to production performance (Webster and Czarick, 2000), making it critical to evaluate spatial thermal distribution. Longitudinal, lateral, vertical, and within/between colony rows spatial dimensions of temperature and relative humidity are summarized in Table 4.

Laterally, Columns 1 and 3 showed symmetrical temperature profiles ($P > 0.05$), which may be attributed to the external sunshade structure. Column 2 had an average temperature 0.7 °C lower than the sides ($P < 0.05$). This observation aligns with the findings of Trokhaniak et al. (2023) and Tian et al. (2024), the downward deflection of inlet jets following roof impingement at the center creates a localized low-temperature zone in the middle column, enhancing the airflow circulation within the animal-occupied zone.

Longitudinally, no significant temperature variations were observed between the front and middle sections ($P > 0.05$). The rear section exhibited 0.4°C higher average temperature than the front and middle regions ($P < 0.05$). This difference can be explained by the placement of the evaporative cooling pads in the front two-thirds of the buffer space, which directly influenced the intake temperature. Additionally, fan extraction in the rear section partially suppressed the Coandă effect of airflow, leading to increased air turbulence (Babadi et al., 2022).

Table 4
Spatial distribution (mean ± SD) of indoor temperature and relative humidity during July 2024.

Locations	Temperature (°C)	Relative Humidity (%)
Front	26.1 ± 1.67 [b]	80 ± 3.6 [c]
Middle	26.2 ± 1.62 [b]	82 ± 4.5 [a]
Rear	26.5 ± 1.73 [a]	81 ± 4.9 [b]
Column 1	26.7 ± 1.61 [a]	83 ± 3.7 [a]
Column 2	26.0 ± 1.69 [b]	82 ± 4.2 [b]
Column 3	26.7 ± 1.44 [a]	80 ± 5.1 [c]
Tier 1	26.4 ± 1.70 [ab]	80 ± 4.5 [c]
Tier 2	26.1 ± 1.66 [b]	83 ± 3.5 [a]
Tier 3	26.5 ± 1.65 [a]	82 ± 4.6 [b]
Tier 4	25.7 ± 1.48 [c]	83 ± 4.1 [a]
Between Colony Rows	26.5 ± 1.29	80 ± 5.5
Within Colony Rows	28.0 ± 1.62	71 ± 5.9

Note: The different superscript letters ("a", "b", and "c") indicate that the means (± SD) in the same column (along the longitudinal, lateral, and vertical direction, respectively) differ ($P < 0.05$); the same were no significant differences.

Vertically, temperatures within the housing system ranked from highest to lowest as follows: Tier 3 > Tier 1 > Tier 2 > Tier 4. The heat produced by the birds is a significant driver of the microclimate inside the house, meaning that the distribution of birds across different tiers can influence temperature variations (Chepete et al., 2004). In a multi-tier housing system, bird distribution is highly uneven and not static.

Tier 4, which contains egg-laying boxes, exhibits significantly lower temperatures compared to the other tiers ($P < 0.05$), with a maximum mean temperature difference of 1.1°C relative to Tier 3. This lower temperature is primarily due to reduced bird occupancy, caused by the removal of feeders and drinkers (Yin et al., 2024). Furthermore, the lighting regimen (see Table 2) contributed to the thermal pattern by influencing hen movement. For instance, after the morning laying peak, hens vacated the top-tier nest boxes due to the lack of feed resources, leading to a rapid decline in local biotic heat production. After lights-off, the relocation of most hens to floors and perches further reduced occupancy and heat generation on the upper tiers. Moreover, we observed aggressive behaviors (e.g., pecking) from dominant hens on higher tiers, preventing hens from lower tiers from moving upward, which reinforced the stratification of bird density. Furthermore, we noted aggressive behaviors, such as pecking, from dominant hens on the higher tiers. This aggression prevents hens on the lower tiers from moving up, thereby reinforcing the stratification of bird density. Another important factor contributing to these temperature differences is the cooler incoming air introduced near the top tier. The longitudinal airflow tends to move through the space near the roof, which has lower ventilation resistance, resulting in higher wind speeds at the top tier (Cheng et al., 2018).

Temperatures within the colony rows were significantly higher (28.0 ± 1.62°C) and exhibited greater variability than those found in the interstitial zones between the colony rows (26.5 ± 1.29°C), with an average difference of 1.5°C. This temperature gradient may be influenced by increased airflow resistance and the hens' direct exposure to their own metabolic heat and humidity (Tong et al., 2019; Zheng et al., 2020). However, it is important to note that while temperature and relative humidity were monitored at multiple levels, airflow velocity measurements—which are essential for comparing airflow resistance and evaluating actual heat stress across different farming systems—were not included in this study.

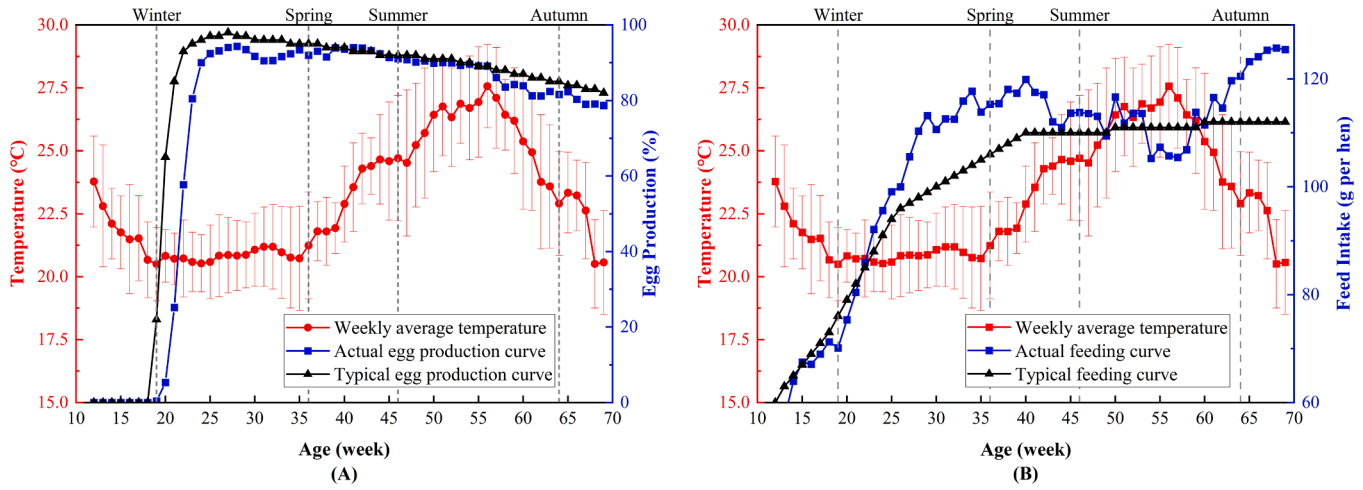

Fig. 9. (A) Egg production and (B) feed intake of *Jing Ting No.6* hens in relation to indoor temperature throughout the production cycle (12-70 weeks).

Flock performance in relation to thermal environment

Fig. 9A compares the weekly laying rate against the theoretical curve provided by the breeder for Jing Ting No.6 hens from 12 to 70 weeks of age. The overall trend of actual egg production broadly aligned with the benchmark curve. Hens commenced laying at 22 weeks of age (50 % production), reached a peak lay of 94 % at 27 weeks, and maintained a laying rate above 85 % until 57 weeks. Weekly feed consumption, as shown in Fig. 9B, followed the expected physiological trend, increasing to a peak of 120.0 g per hen per day at 40 weeks before declining to 105.3 g per hen per day by week 54. The higher activity requirements in the multi-tier system likely increased maintenance energy demands, except during heat stress, when reduced feed intake was observed (De Andrade et al., 1977; Marsden and Morris, 1987; Lin et al., 2016).

However, actual production consistently remained slightly below theoretical values. While the reasons for this discrepancy are unclear, it may be related to management adjustments to the new housing system and behavioral issues, such as pecking and crowding within larger group pens. These factors have been previously linked to lower productivity in multi-tier systems compared to conventional cages (Yilmaz Dikmen et al., 2016; Decina et al., 2019; Erek and Matur, 2024; Shoji et al., 2025). Additionally, although the *Jing Ting* breed is known for its high production levels, our observations suggest it may be more vulnerable to stress in complex aviary environments.

Pearson correlation analysis confirmed that air temperature plays a significant role in influencing the productivity and feed consumption of laying hens (see Table 5), which aligns with established literature (Payne, 1966; Arieli et al., 1980; Peguri and Coon, 1991; Kim et al., 2022b; Li et al., 2024). A positive correlation was found between deviations in egg production and the average daily temperature over the past three days ($P < 0.05$), with the highest correlation coefficient observed for the current daily maximum temperatures. Additionally, feed intake deviations exhibited even stronger negative correlations with thermal parameters. Significant relationships were noted with average daily temperature, maximum temperature, and minimum temperature ($P < 0.001$), and substantial correlation persistence was observed for up to a week after the measurements. Interestingly, diurnal temperature fluctuations on the same day showed only a moderate correlation with feed intake ($P < 0.05$) and no significant correlation with egg production ($P > 0.05$). This lack of correlation may be due to the effective performance of the ASV system, which maintained daily temperature variations within 4.7°C throughout the production cycle—well below the 6°C threshold recommended to minimize productivity loss (Al-Saffar and Rose, 2002). These findings emphasize the importance of implementing thermal management strategies that consider both immediate and delayed effects of temperature, particularly in controlling cumulative heat load to reduce declines in feed intake and subsequent egg production.

Table 5
Pearson's correlations among the 7-day daily average temperature, minimum and maximum temperatures, diurnal temperature fluctuations, egg production, and feed intake.

Item		Egg Production[1] (%)		Feed Intake[2] (g per hen)	
		r[3]	P-value	r	P-value
Current Day	T^4_{min}	0.525***	0.000	−0.789***	0.000
	T^5_{max}	0.540***	0.000	−0.769***	0.000
	T^6_{avg}	0.518***	0.000	−0.795***	0.000
	ΔT^7	0.212ns	0.153	−0.314*	0.032
Prior-Day	T_{min}	0.458**	0.001	−0.799***	0.000
	T_{max}	0.427**	0.003	−0.752***	0.000
	T_{avg}	0.429**	0.003	−0.784***	0.000
	ΔT	0.149ns	0.317	−0.276ns	0.060
Two-Day Prior	T_{min}	0.365*	0.012	−0.754***	0.000
	T_{max}	0.383**	0.008	−0.692***	0.000
	T_{avg}	0.361*	0.013	−0.729***	0.000
	ΔT	0.240ns	0.104	−0.241ns	0.103
Three-Day Prior	T_{min}	0.277ns	0.060	−0.747***	0.000
	T_{max}	0.328*	0.024	−0.664***	0.000
	T_{avg}	0.297*	0.042	−0.698***	0.000
	ΔT	0.283ns	0.054	−0.202ns	0.173
Four-Day Prior	T_{min}	0.276ns	0.060	−0.677***	0.000
	T_{max}	0.288*	0.050	−0.585***	0.000
	T_{avg}	0.252ns	0.088	−0.643***	0.000
	ΔT	0.182ns	0.220	−0.137ns	0.359
Five-Day Prior	T_{min}	0.206ns	0.165	−0.608***	0.000
	T_{max}	0.229ns	0.121	−0.533***	0.000
	T_{avg}	0.186ns	0.212	−0.577***	0.000
	ΔT	0.176ns	0.237	−0.141ns	0.344
Six-Day Prior	T_{min}	0.126ns	0.400	−0.540***	0.000
	T_{max}	0.149ns	0.319	−0.484***	0.001
	T_{avg}	0.102ns	0.496	−0.497***	0.000
	ΔT	0.131ns	0.382	−0.153ns	0.306

Note: [1]The deviation of actual production performance from theoretical values; [2]The deviation of actual feed intake from theoretical values; [3]The Pearson's correlation; [4]The daily minimum temperature; [5]The daily maximum temperature; [6]The daily average temperature; [7]The diurnal temperature fluctuations; *$P < 0.05$; **$P < 0.01$; ***$P < 0.001$; ns, no significant ($P > 0.05$).

Conclusion

An ASV system with buffer spaces and constant air inlets was developed to stabilize the incoming airflow and minimize the temperature fluctuation under diverse seasonal and weather extremes. The

following conclusions were based on a comprehensive evaluation conducted in a 24,000-hen commercial multi-tier layer house under a temperate monsoon climate over a full production cycle:

1. The ASV system maintained indoor temperatures within 18.3-29.8°C throughout the production cycle, with daily temperature fluctuation controlled within 3°C for 77.4 % of the time and never exceeding 4.7°C regardless of seasonal variations.
2. The system kept the indoor temperature at 18.3°C without supplemental heating when outdoor temperatures dropped to −22.0°C, while maintaining a stocking density of 0.064 m^2 per hen.
3. The ASV system demonstrated effective progressive thermal buffering ($P < 0.05$), reducing a 21.9 °C outdoor diurnal fluctuation to 17.7 °C in the buffer spaces, 12.2 °C at the inlets, and only 4.7 °C indoors.
4. Spatial analysis revealed significant thermal variation: longitudinally, higher temperatures in the rear section; laterally, a 0.7°C cooler central column; vertically, the highest temperature on Tier 3 and the lowest on Tier 4; and a 1.5°C temperature increase with 9 % lower relative humidity within colony rows ($P < 0.05$).
5. Diurnal feed intake deviation strongly negatively correlated with 7-day mean, maximum, and minimum indoor temperatures, whereas egg production deviation showed a strong positive correlation with the current day's mean, maximum, and minimum temperatures ($P < 0.001$).

CRediT authorship contribution statement

Y.J. Chen: Conceptualization, Data curation, Formal analysis, Investigation, Methodology, Supervision, Validation, Visualization, Writing – original draft, Writing – review & editing. **S.Z. Deng:** Conceptualization, Formal analysis, Methodology, Software, Writing – original draft. **Y. Wang:** Conceptualization, Formal analysis, Funding acquisition, Methodology, Writing – review & editing. **C. Liu:** Conceptualization, Formal analysis, Methodology, Validation, Writing – original draft, Writing – review & editing. **W.X. Qin:** Data curation, Project administration. **Y.X. Wei:** Data curation, Project administration, Supervision. **Q. Tong:** Funding acquisition, Writing – review & editing. **B. M. Li:** Conceptualization, Funding acquisition, Project administration, Resources, Writing – review & editing. **W.C. Zheng:** Conceptualization, Funding acquisition, Project administration, Resources, Supervision, Validation, Writing – original draft, Writing – review & editing.

Disclosures

The authors declare that they have no known competing financial interests or personal relationships that could have appeared to influence the work reported in this paper.

Acknowledgements

All experiment procedures involving the use of animals in this experiment were reviewed and approved by the Laboratory Animal Ethical Committee of China Agricultural University (AW52114202-6-01). Funding for this study was provided by the National Key R&D Program of China (2023YFD200080401), the National Natural Science Foundation of China (32272924), and the China Agriculture Research System of MOF and MARA (CARS-40). Additionally, we extend our thanks to our colleagues at the Key Laboratory of Agricultural Engineering in Structure and Environment, China Agricultural University, Beijing, China.

References

Albright, L.D., Scott, N.R., 1974. An analysis of steady periodic building temperature variations in warm weather part I: a mathematical model. Trans. ASABE. 17 (1), 88–92.
Al-Saffar, A.A., Rose, S.P., 2002. Ambient temperature and the egg laying characteristics of laying fowl. World's Poult. Sci. J. 58 (3), 317–331.
Arieli, A., Meltzer, A., Berman, A., 1980. The thermoneutral temperature zone and seasonal acclimatisation in the hen. Br. Poult. Sci. 21, 471–478.
Babadi, K.A., Khorasanizadeh, H.., Aghaei, A.A., 2022. CFD modeling of air flow, humidity, CO_2 and NH_3 distributions in a caged laying hen house with tunnel ventilation system. Comput. Electron. Agric. 193, 106677.
Barrett, N.W., Rowland, K.., Schmidt, C.J., Lamont, S.J., Rothschild, M.F., Ashwell, C.M., Persia, M.E., 2019. Effects of acute and chronic heat stress on the performance, egg quality, body temperature, and blood gas parameters of laying hens. Poult Sci 98 (12), 6684–6692.
Bjerg, B., Svidt, K., Zhang, G., Morsing, S., Johnsen, J.O., 2002. Modeling of air inlets in CFD prediction of airflow in ventilated animal houses. Comput. Electron. Agric. 34 (1–3), 223–235.
Chen, Y., Raphael, B., Sekhar, S.C., 2016. Experimental and simulated energy performance of a personalized ventilation system with individual airflow control in a hot and humid climate. Build. Environ. 96, 283–292.
Chen, L., Fabian-Wheeler, E.E., Cimbala, J.M., Hofstetter, D., Patterson, P.H., 2021. Computational fluid dynamics analysis of alternative ventilation schemes in cage-free poultry housing. Animals (Basel) 11 (8), 2352.
Chen, Y., L. Zhao, H. He, X. Lin, H. Zeng, Z. Wu, Y. Jiang, and Y. Li. 2022. GB/T 42074-2022. Division of climatic seasons. State general administration of the People's Republic of China for quality supervision and inspection and quarantine. (In Chinese).
Cheng, Q., Li, H., Rong, L., Feng, X., Zhang, G., Li, B., 2018. Using CFD to assess the influence of ceiling deflector design on airflow distribution in hen house with tunnel ventilation. Comput. Electron. Agric. 151, 165–174.
Chepete, H.J., Puma, M..C., Xin, H., Gates, R.S., 2004. Heat and moisture production of poultry and their housing systems: pullets and layers. ASHRAE Trans 110 (2), 286–299.
Choi, L., Daniel, K., Lee, S., Lee, C., Park, J., Park, J., Hong, S., 2024. CFD simulation of dynamic temperature variations induced by tunnel ventilation in a broiler house. Animals (Basel) 14 (20), 3019.
Dawkins, M.S., Donnelly, C..A., Jones, T.A., 2004. Chicken welfare is influenced more by housing conditions than by stocking density. Nature 427 (6972), 342–344.
De Andrade, A.N., Rogler, J..C., Featherston, W.R., Alliston, C.W., 1977. Interrelationships between diet and elevated temperatures (cyclic and constant) on egg production and shell quality. Poul. Sci. 56, 1178–1977.
Decina, C., Berke, O., Staaveren, N.V., Baes, C.F., Widowski, T.M., Harlander-Matauschek, A., 2019. A cross-sectional study on feather cover damage in Canadian laying hens in non-cage housing systems. BMC Vet. Res. 15 (1), 435.
Erek, M., Matur, E., 2024. Effects of housing systems on production performance, egg quality, tonic immobility and feather score in laying hens. Vet. Med. Sci. 10 (6), e70112.
Fu, S.F., 2019. MS Thesis. China Agric. Univ., Beijing.
Garcimartin, M.A., Ovejero, I.., Sanchez, E., SáNCHEZ-GIRóN, V., 2007. Application of the sensible heat balance to determine the temperature tolerance of commercial poultry housing. World's Poult. Sci. J. 63 (4), 575–584.
Gebremedhin, K.G., Wu, B., 2005. Simulation of flow field of a ventilated and occupied animal space with different inlet and outlet conditions. J. Therm. Biol. 30 (5), 343–353.
Han, J., Fang, S., Wang, X., Zhuo, W., Yu, Y., Peng, X., Zhang, Y., 2024. The impact of intra-annual temperature fluctuations on agricultural temperature extreme events and attribution analysis in mainland China. Sci. Total Environ. 949, 174904.
Harris J.r., G.C., Dodgen, W.H., Nelson, G.S., 1974. Effects of diurnal cyclic growing temperatures on broiler performance. Poult. Sci. 53 (6), 2204–2208.
Hayes, M.D., Xin, H.., Li, H., Shepherd, T.A., Zhao, Y., Stinn, J.P., 2013. Heat and moisture production of hy-line brown hens in aviary houses in the. Midwestern U.S. Trans. ASABE. 56 (2), 753–761.
Hong, E., Kang, H., Jeon, J., You, A., Kim, H., Son, J., Kim, H., Yun, Y., Kang, B., Kim, J., 2021. Studies on the concentrations of particulate matter and ammonia gas from three laying hen rearing systems during the summer season. J. Environ. Sci. Heal. B. 56 (8), 753–760.
Howlider, M.A.R., Rose, S.P., 1987. Temperature and the growth of broilers. World's Poult. Sci. J. 43 (3), 228–237.
Hui, X., Li, B., Xin, H., Zheng, W., Shi, Z., 2018. New control strategy against temperature sudden-drop in the initial stage of pad cooling process in poultry houses. Int. J. Agr. Biol. Eng. 11 (1), 66–73.
Kim, J., Lee, I.B., Lee, S., Park, S., Jeong, D., Choi, Y., Decano-Valentin, C., Yeo, U., 2022a. Development of an air-recirculated ventilation system for a piglet house, part 1: analysis of representative problems through field experiment and aerodynamic analysis using CFD simulation for evaluating applicability of system. Agriculture (Basel) 12 (8), 1139.
Kim, D., Lee, Y., Lee, S., Lee, K., 2022b. Impact of relative humidity on the laying performance, egg quality, and physiological stress responses of laying hens exposed to high ambient temperature. J. Ther. Biol. 103, 103167.
Kim, D.H., Song, J..Y., Park, J., Kwon, B.Y., Lee, K.W., 2023. The effect of low temperature on laying performance and physiological stress responses in laying hens. Animals (Basel) 13 (24), 3824.

Kindangen, J.I., Rogi, O..H., Gosal, P.H., Kumurur, V.A., 2022. Attic ventilation and radiant heat barriers in naturally ventilated galvanized metal-roofed buildings. Adv. Build. Energy Res. 16 (5), 669–695.
Kwon, K., Lee, I., Zhang, G., Ha, T., 2015. Computational fluid dynamics analysis of the thermal distribution of animal occupied zones using the jet-drop-distance concept in a mechanically ventilated broiler house. Biosyst. Eng. 136, 51–68.
Li, Z., Wang, C., Li, B., Shi, Z., Zheng, W., Teng, G., 2020. Concentration and size distribution of particulate matter in a new aviary system for laying hens in China. J. Air. Waste. Manag. Assoc. 70 (4), 379–392.
Li, Z., Xiong, Y., Wang, S., Wang, C., Ji, B., Liu, Y., Liang, C., Tong, Q., 2023. Assessing particulate matter concentration level and its limit exceedance based on year-round field measurements of different laying hen building systems. Biosyst. Eng. 226, 266–279.
Li, Y., Ma, R., Qi, R., Li, H., Li, J., Liu, W., Wan, Y., Liu, Z., Li, S., Chang, X., Yuan, Z., Liu, X., Wang, X., Zhan, K., 2024. Study on the changing patterns of production performance of laying hens and their relationships with environmental factors in a large-scale henhouse. Poult. Sci. 103 (11), 104185.
Lin, X., Zhang, R., Jiang, S., Elmashad, H.M., Mitloehner, F., 2016. Nutrient flow and distribution in conventional cage, enriched colony, and aviary layer houses. Poult. Sci. 95 (1), 213–224.
Luo, Z., Liu, J., Zhang, Y., Zhou, J., Shao, W., Yu, Y., Jia, R., 2021. Seasonal variation of dry and wet islands in Beijing considering urban artificial water dissipation. npj Clim. Atmos. Sci. 4, 58.
Lysenko, V., Golovinskiy, B., Reshetyuk, V., Golub, B., Shcherbatyuk, V., 2011. Dynamics of quality indexes of laying hens keeping process due to fluctuations of temperature disturbances in an industrial poultry house. Ann. Wars. Univ. Life Sci.-SGGW. 57, 79–92.
Marsden, A., Morris, T.R., 1987. Quantitative review of the effects of environmental temperature on food intake, egg output and energy balance in laying pullets. Brit. Poultry Sci. 28, 693–704.
Mueller, W.J., 1961. The effect of constant and fluctuating environmental temperatures on the biological performance of laying pullets. Poult. Sci. 40 (6), 1562–1571.
Olgun, M., Çelik, M.Y., Polat, H.E., 2007. Determining of heat balance design criteria for laying hen houses under continental climate conditions. Build. Environ. 42 (1), 355–365.
Oliveira, J.L., Ramirez, B..C., Xin, H., Wang, Y., Hoff, S.J., 2020. Ventilation performance and bioenergetics of dekalb white hens in a modern aviary system. Biosyst. Eng. 199, 149–161.
Payne, C.G., 1966. Practical aspects of environmental temperature for laying hens. World's Poult. Sci. J. 22 (2), 126–139.
Peguri, A., Coon, C., 1991. Effect of temperature and dietary energy on layer performance. Poult. Sci. 70 (1), 126–138.
Predicala, B.Z., Maghirang, R.G., 2003. Numerical simulation of particulate matter emissions from mechanically ventilated swine barns. Trans. ASABE. 46 (6), 1685–1694.
Randall, J.M., Battams, V.A., 1979. Stability criteria for airflow patterns in livestock buildings. J. Agric. Eng. Res. 24 (4), 361–374.
Rehman, M.S., Mahmud, A.., Mehmood, S., Pasha, T.N., Khan, M.T., Hussain, J., 2018. Assessing behavior in Aseel pullets under free-range, part-time free-range, and cage system during growing phase. Poult. Sci. 97 (3), 725–732.
Ruzal, M., Shinder, D., Malka, I., Yahav, S., 2011. Ventilation plays an important role in hens' egg production at high ambient temperature. Poult. Sci. 90 (4), 856–862.
Sandberg, M., Moshfegh, B., 1998. Ventilated-solar roof air flow and heat transfer investigation. Renew. Energ. 15 (1–4), 287–292.
Säwén, T., Stockhaus, M., Hagentoft, C.E., Schjøth Bunkholt, N., Wahlgren, P., 2021. Model of thermal buoyancy in cavity-ventilated roof constructions. J. Build. Phys. 45 (4), 413–431.
Shoji, G.R.T., Sekizawa, S., Kuwahara, M., 2025. Evaluation of physiological functions and production performance in laying hens in three different housing systems. Poult. Sci. 104, 105256.
Tao, X.P., 2003. Effects of temperature-humidity-velocity conditions on the sensitive physiological and biochemical indices of broilers. Chinese Acad. Agric. Sci.
Tian, X., Yin, H., Ji, D., Zhao, W., Shang, T., Hu, Z., Li, A., 2024. Airflow collision characteristics of double square column attachment ventilation. Build. Environ. 260, 111696.
Tong, X., Hong, S., Zhao, L., 2019. CFD modeling of airflow, thermal environment, and ammonia concentration distribution in a commercial manure-belt layer house with mixed ventilation systems. Comput. Electron. Agric. 162, 281–299.
Trokhaniak, V., Gorobets, V., Shutyi, O., Dubrovina, O., 2023. Investigation of the side ventilation system in the poultry house using CFD. Mech. Agric. Conserv. Resour. 67 (5), 154–157.
Turner, I., Heidari, D., Pelletier, N., 2022. Life cycle assessment of contemporary Canadian egg production systems during the transition from conventional cage to alternative housing systems: update and analysis of trends and conditions. Resour. Conserv. Recy. 176, 105907.
Wang, F., 2012. MS Thesis. China Agric. Univ., Beijing.
Wang, Y., Zheng, W., Tong, Q., Li, B., 2018a. Reducing dust deposition and temperature fluctuations in the laying hen houses of Northwest China using a surge chamber. Biosyst. Eng. 175, 206–218.
Wang, Y., Zheng, W., Shi, H., Li, B., 2018b. Optimising the design of confined laying hen house insulation requirements in cold climates without using supplementary heat. Biosyst. Eng. 174, 282–294.
Wang, Y., Zheng, W., Li, B., Li, X., 2019. A new ventilation system to reduce temperature fluctuations in laying hen housing in continental climate. Biosyst. Eng. 181, 52–62.
Wang, Y., 2020. Temperature stability mechanism and thermal environment regulation for healthy and efficient poultry stocking. PhD Diss. China Agric. Univ.
Webster, A.B., Czarick, M., 2000. Temperatures and performance in a tunnel-ventilated, high-rise layer house. J. Appl. Poult. Res. 9 (1), 118–129.
Xu, M.J., 2022. MS Thesis. China Agric. Univ., Beijing.
Yang, Z., Tu, Y., Ma, H., Yang, X., Liang, C., 2021. Numerical simulation of a novel double-duct ventilation system in poultry buildings under the winter condition. Build. Environ. 207 (Part B), 108557.
Yang, X., Bist, R., Paneru, B., Chai, L., 2024. Monitoring activity index and behaviors of cage-free hens with advanced deep learning technologies. Poult. Sci. 103 (11), 104193.
Yeo, U., Lee, I., Kim, R., Lee, S., Kim, J., 2019. Computational fluid dynamics evaluation of pig house ventilation systems for improving the internal rearing environment. Biosyst. Eng. 186, 259–278.
Yilmaz Dikmen, B., İpek, A., Şahan, Ü., Petek, M., Sözcü, A., 2016. Egg production and welfare of laying hens kept in different housing systems (conventional, enriched cage, and free range). Poult. Sci. 95 (7), 1564–1572.
Yin, P., Tong, Q., Li, B.M., Zheng, W.C., Wang, Y., Peng, H.Q., Xue, X.L., Wei, S.Q., 2024. Spatial distribution, movement, body damage, and feather condition of laying hens in a multi-tier system. Poult. Sci. 103 (1), 103202.
Zhao, Y., Xin, H., Shepherd, T., Hayes, M., Stinn, J., 2013. Modeling ventilation rate, balance temperature and supplemental heat need in alternative vs. conventional laying-hen housing systems. Biosyst. Eng. 115 (3), 311–323.
Zhao, Y., Shepherd, T.A., Li, H., Xin, H., 2015. Environmental assessment of three egg production systems–Part I: monitoring system and indoor air quality. Poult. Sci. 94 (3), 518–533.
Zheng, W., Xiong, Y., Gates, R.S., Wang, Y., Koelkebeck, K.W., 2020. Air temperature, carbon dioxide, and ammonia assessment inside a commercial cage layer barn with manure-drying tunnels. Poult. Sci. 99 (8), 3885–3896.